LANGMUIR

Invited Feature Article

pubs.acs.org/Langmuir

Balancing Segregation and Complexation in Amphiphilic Copolymers by Architecture and Confinement

Pascal Hebbeker, Alexander A. Steinschulte, Stefanie Schneider, and Felix A. Plamper*

Institute of Physical Chemistry II, RWTH Aachen University, Landoltweg 2, 52056 Aachen, Germany

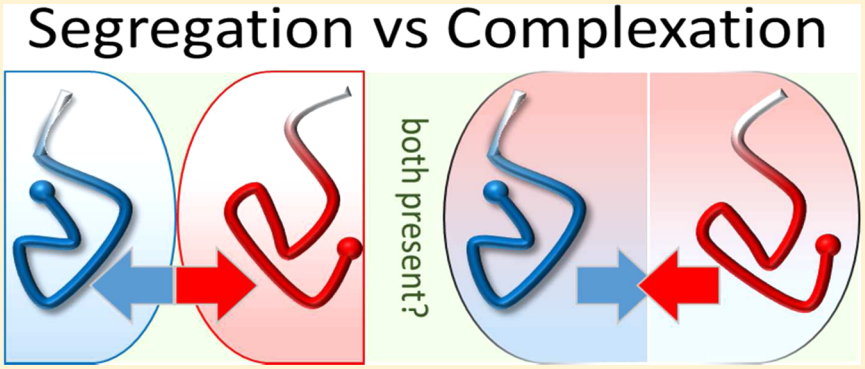

ABSTRACT: Segregation is a well-known principle for micellization, as solvophobic components try to minimize interactions with other entities (such as solvent) by self-assembly. An opposite principle is based on complexation (or coacervation), leading to the coassembly/association of different components. Most cases in the literature rely on only one of these modes, though the classical micellization scheme (such as spherical micelles, wormlike micelles, and vesicles) can be enriched by a subtle balance of segregation and complexation. Because of their counteraction, micellar constructs with unprecedented structure and behavior could be obtained. In this feature, systems are highlighted, which are between both mechanisms, and we study concentration, architecture, and confinement effects. Systems with inter- and intramolecular interactions are presented, and the effects of polymer topology and monomer sequence on the resulting structures are discussed. It is shown that complexation can lead to altered micellization behavior as the complex of one hydrophobic and one hydrophilic component can have a very low surface tension toward the solvent. Then, the more soluble component is enriched at the surface of the complex and acts as a microsurfactant. Although segregation dominates for amphiphilic copolymers in solution, the effect of the complexation can be enhanced by branching (change of architecture). Another possibility to enhance the complexation is by confining copolymers in a (pseudo-) 2D environment (like the one available at liquid−liquid interfaces). These observations show how new structural features can be achieved by tuning the subtle balance between segregation and complexation/solubilization.

INTRODUCTION

The aim of this feature article is to discuss complexation and segregation and to illustrate their interplay. These principles are essential for polymer and soft matter systems, radiating even to the very heart of biological systems: life is sustained by both complexation (e.g., double helix of DNA) and segregation (e.g., lipid bilayer of the cell wall). Though both principles can be present in the same system (such as a cell), a competing scenario between both principles is rarely encountered. In the following text, we introduce both concepts and discuss possible consequences in a well-balanced system, where both complexation and segregation compete. The understanding and exploitation of interactions between polymer chains is one of the most crucial aspects in polymer science. Polymer interactions affect all areas in polymer physics, with far-reaching effects on material properties such as solubility,[1] compatibility/miscibility,[2] mobility,[3] mechanical properties,[4] and the glass-transition temperature (T_g).[5]

Depending on the interactions that are present in the system, mixtures of polymers, both in the melt and in solution, can show segregative behavior as well as associative behavior (complexation). If a polymer preferentially interacts with its own type, then it phase separates (or microphase separates in the case of copolymers) by segregation. On the other hand, if the polymer shows a stronger effective attraction toward entities other than its own type, then mixing is observed. Generally, this scenario can be comprehended as a complexation-driven one. In our context, we specifically ascribe the notion complexation to the preferential interaction of polymers with other polymers (or at least to the preferential interaction of polymers with entities other than solvent[6−16]).

The preferential interaction of polymers with solvent molecules can be best described as solubilization (though the underlying principles are the same for complexation and solubilization[17,18]). Then, not only the interaction of the polymer segments with each other but also the interaction of

Received: December 22, 2016
Revised: February 11, 2017
Published: February 21, 2017

DOI: 10.1021/acs.langmuir.6b04602
Langmuir 2017, 33, 4091−4106

the polymer segments with the solvent has an effect on the self-assembly. For example, in the case of segregating polymers in solution, self-assembly into micellar aggregates is observed for amphiphilic (block) copolymers.

By balancing the coexistence of segregation, complexation, and solubilization, deviations from the classical equilibrium micellization scheme of amphiphilic copolymers (strongly segregated blocks with clearly defined interfaces) are expected. Therefore, the interplay of complexation/segregation/solubilization could provide a pathway to new equilibrium micellar/colloidal structures (such as core−shell−corona structures) and functionalities, which would not be accessible otherwise for conventional binary copolymer systems.

In the following text, we explain the principles of segregation and complexation and their possible balancing in more detail.

Segregation. When considering different polymers in the melt, they are only rarely miscible. By combining the enthalpic and entropic terms of an expanded regular solution theory, the Flory−Huggins theory provides tools for understanding the polymer miscibility in polymer blends.[19] The theory shows that the mixing entropy vanishes for reasonable degrees of polymerization. Because any nonspecific interactions (e.g., London dispersion forces) energetically favor demixing, segregation takes place.

In addition to the demixing of polymers in the melt, the Flory−Huggins theory also rationalizes the selectivity of solvents. An extension of the theory also allows the rationalization of the thermosensitive behavior of polymers.[20] The selectivity of the solvent leads to segregation and the formation of the structures that are well known from the classical micellization scheme.

An illustration is the self-assembly of block copolymers in solution into various micellar morphologies, as the use of selective solvents can lead to microphase separation of the insoluble component(s) of the polymer. This process is driven by segregation, as segregating polymers try to minimize the number of contacts with other components (such as solvent) but want to maximize the number of contacts with entities of their own type. The shape of the self-assembled structure is dictated by the polymer architecture such as the ratio of the different block lengths in block copolymers. As a consequence, spherical, star-shaped micelles (core/corona-type micelles), wormlike micelles, or vesicular micelles are observed in solution/dispersion by the use of diblock copolymers.[21] The formation of such equilibrium structures is rather well understood from a theoretical point of view by considering the contributions of the polymer coil stretching in the insoluble part, the contribution of steric interactions of solvated chains in the corona, and the contributions from interfacial effects.[22]

Many water-soluble polymers phase separate from a homogeneous solution with increasing temperature. The lowest possible temperature at which phase separation can occur is called the lower critical solution temperature, LCST.[23] Such behavior is often ascribed to the entropic gain upon release of structured water molecules, which are located around polymeric hydrocarbon moieties at low temperature. One of the most prominent and well-studied examples among the LCST-type polymers in aqueous media is poly(*N*-isopropylacrylamide) PNIPAM.[24] But poly(propylene oxide) PPO (often called also poly(propylene glycol) PPG), poly(*N*,*N*-diethyl acrylamide) PDEAAM,[18] and poly(2-(dimethylamino)ethyl methacrylate) PDMAEMA also belong to the class of LCST-type polymers in water. For PPO, the phase transition occurs typically below room temperature (dependent on concentration and molecular weight),[23] whereas PDMAEMA can have phase-transition temperatures far above room temperature (low pH increases the cloud points beyond the experimentally accessible region).[25]

Complexation. Even though, according to Flory−Huggins theory, polymer melts favor demixing, some examples of miscible polymer couples are known (without microphase separation), such as the PPO/PDMAEMA couple.[26] This miscibility is due to specific attractive interactions between the *different* monomers (having anchor groups for pronounced ionic or hydrogen bonding; see also below). Hence, we call such resulting species complexes or coacervates (in the case of liquidlike behavior; in the following text, we stick to the notion "complex").[27]

We briefly describe the different types of interactions that can lead to complexation: ionic, H-bonding, and van der Waals attraction (including dipole−dipole interactions). Here, long-ranged ionic bonding is one of the most prominent types of interaction. An interpolyelectrolyte complex (IPEC)[28] is formed by the mixing of two oppositely charged polyelectrolytes (which are polymers with multiple charges along the chain).[29−35] The major driving force for complexation can be traced back to the entropic gain due to the release of counterions. As an alternative to ionic bonding, hydrogen bonding is another effective way to marry two different polymers. As classic examples, protonated poly((meth)acrylic acid) (P(M)AA) forms insoluble complexes with poly(ethylene oxide) (PEO),[36] poly(vinyl methyl ether), or poly(4-vinylpyridine).[37] P(M)AA is an effective hydrogen bond donor, interacting also with other hydrogen bond acceptors such as poly(acrylamides).[38,39] Although PNIPAM is immiscible with structurally similar poly(vinylpyrrolidone), it forms strong complexes with PAA. Hence, PNIPAM, which as a secondary amide can be both an H-bond acceptor and donor, has less H-bond donor ability than PAA. Still, in some cases the H-bond donor abilities are visible when being offered a more effective H-bond acceptor such as poly(*N*,*N*-diethyl acrylamide) (PDEAAM).[40] As a tertiary amide, PDEAAM cannot act as an H-bond donor, but the two ethyl groups donate inductively electron density to the amide bond. Similar effects were observed for poly(*N*-vinyl caprolactam) PVCl and PNIPAM.[41] Architectural effects on PNIPAM/PDEAAM complexation will be discussed in the main part.

For more unusual combinations such as poly(styrene) and poly(vinyl methyl ether),[42] poly(styrene) and poly(phenylene oxide),[43] and poly(methyl methacrylate) and poly(vinylidene fluoride),[44] the van der Waals attraction (including dipolar interactions) can be considered to be an origin of miscibility.

Compared to a polymer melt, the situation is even more multifaceted in solution. First, the effective interaction potentials are altered in solution/dispersion by solvent−polymer interactions compared to the bulk polymer state. We need to differentiate between strongly and weakly interacting components. The transition occurs on the order of k_BT for single bead/bead interactions, as will be discussed later. During complexation, two entities of different polymers form non-covalent bonds, which lead to hardly hydrated (and often insoluble) products. Here, an attractive polymer−polymer interaction must be present as a prerequisite for the creation of such bonds. Then, solvent−polymer contacts can be replaced by favorable polymer−polymer contacts, while the original constituents (e.g., the homopolymers) might be soluble

DOI: 10.1021/acs.langmuir.6b04602
Langmuir 2017, 33, 4091−4106

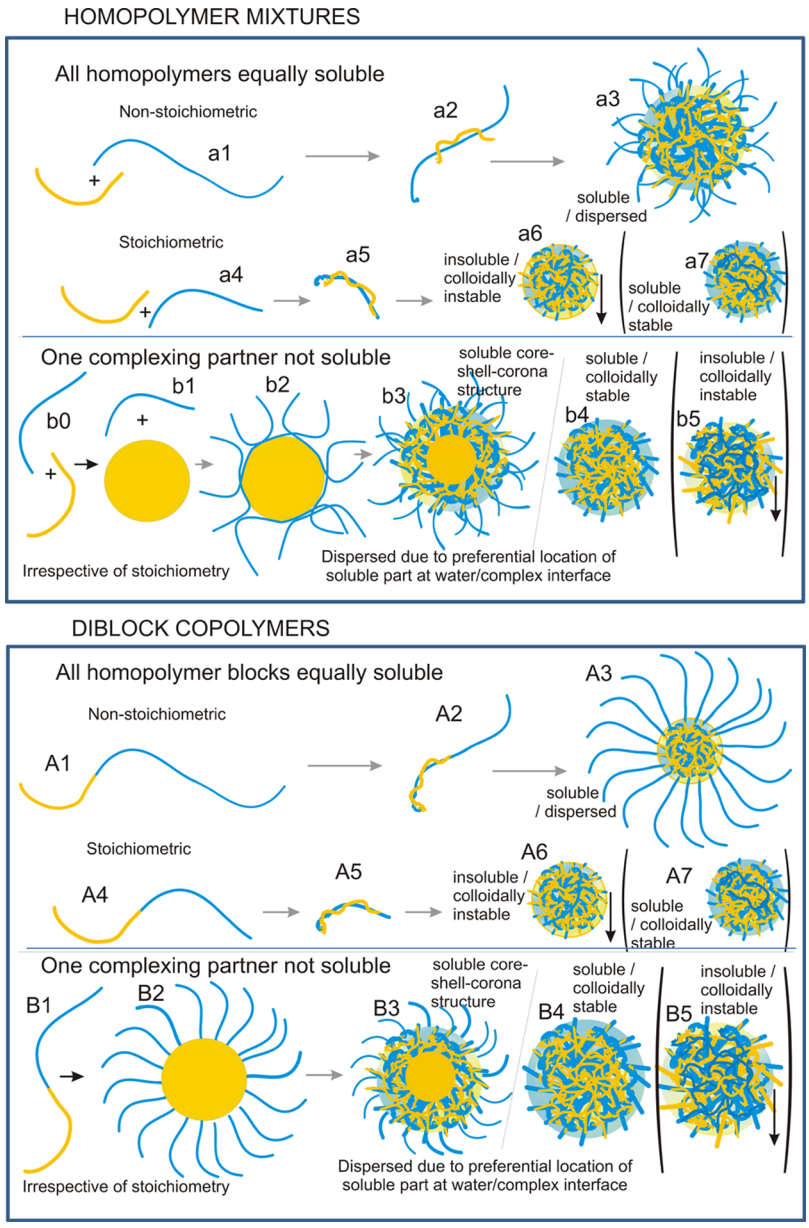

Figure 1. Possible micellar/colloidal structures obtained after the complexation of one polymer partner with the other part in homopolymer mixtures (top, a/b cases) and diblock copolymer examples (bottom, A/B cases). Only linear polymers and core/corona-type micelles are shown for tutorial simplicity (excluding possible branched polymers or wormlike/vesicular morphologies/transitions, which would further broaden the micellization scheme). For the amphiphilic block copolymers, the actual complexation depends on the interaction energy compared to the interplay of segregation strength and entropic conformational penalty due to corona chain folding. Completely insoluble polymer systems, such as stereocomplexes of poly(lactide)s, are not depicted here.

under the same conditions. Often, the solubilizing groups take part in polymer complexation (such as ionic groups or hydrogen bonding entities), aggravating the solubility and facilitating the precipitation of the complex.

In the following, we call the ratio of the polymeric components taking part in the complex the complex composition. A complex in which the complex composition leads to the highest thermodynamic gain is called a stoichiometric complex. This is typically the case when each bond donor has been offered one bond acceptor.

Balancing Complexation and Segregation. After the introduction of segregation and complexation, we anticipated that both effects are antagonistic: complexation counteracts segregation.[45] They are mechanistically rather different, which can be seen when comparing their phase diagrams.[45]

As addressed before, a specific attraction between the polymers is required for the complex formation. Still, segregation can occur as a result of solvent selectivity. Hence, possible scenarios of amphiphilic systems will be addressed in the following list alongside nonamphiphilic systems. For simplicity we focus on cases in the absence of any non-interacting, solubilizing polymer blocks (such as PEO in the case of interpolyelectrolyte complexation/IPEC formation).[30] Then, the following different general scenarios of binary mixtures of attractive (complex forming) polymeric components in (selective) solvent need to be distinguished:

DOI: 10.1021/acs.langmuir.6b04602
Langmuir 2017, 33, 4091−4106

- Solvophilic case: The homopolymers/blocks are equally soluble (a/A cases in Figure 1):
  - Nonstoichiometric complexes (with possible structures a2, a3, A2, and A3 in Figure 1):
    - One of the polymers/blocks in excess provides solubility/colloidal stability of the insoluble complex (IPECs,[31,33] some hydrogen-bonded polymer,[46] and copolymers of NIPAM and DEAAM within a certain temperature region[40])
  - Stoichiometric complexes (structures a5, a6, a7, A5, A6, and A7 in Figure 1):
    - Good colloidal stability/solubility of the complex is provided by the solubilizing effect of the complexed partners, which stay at the surface of the complex (structure a7/A7, Figure 1)
    - Poor colloidal stability/solubility due to attractive interactions between interacting polymer components of different colloidal entities (shown for rather strong complexes such as IPECs[28] but also for weaker complexes between units of NIPAM- and DEAAM-containing copolymers within a certain temperature region;[40] structure a6/A6, Figure 1)
- Case of differing solubilities (amphiphilic case): One polymer/block is soluble, and the other is insoluble (b/B cases in Figure 1 with possible core−shell−corona structures b3/B3 due to balanced segregation/complexation):
  - Nonstoichiometric complexes with soluble major component:
    - Excess soluble polymer/block provides solubility/colloidal stability of the insoluble complex (one example is the complexation between PPO and PDMAEMA in the heat,[47] as shown below; structures b2, b3/B3, and b4/B4 in Figure 1)
  - Stoichiometric complexes and nonstoichiometric complexes with an insoluble major component:
    - Colloidal stability/solubility of the complex is provided by the solubilizing effect of the complexed partner, which stays at the surface of the complex (PPO/PDMAEMA is such an example;[47] structures b2, b3/B3, and b4/B4 in Figure 1).
    - Poor colloidal stability/solubility due to attractive interactions between interacting polymer components of different colloidal entities (structure b5/B5 in Figure 1)
- Solvophobic case: Both homopolymers/blocks are insoluble. Here, most complexes are also insoluble (prominent examples are stereocomplexes, as for PMMA[48] or poly(lactide)s[49])

A summary of the basic scenarios for exemplary homo- and copolymers is depicted in Figure 1.

The above-mentioned list and Figure 1 discuss the possible interplay between segregation and complexation, as could happen in solution-based systems. Binary polymer melt mixtures lack such variety, though weakly segregating systems might have similar features.[50,51] Considering the solvophilic component, there can be a competition between solubilization and complexation for polymer systems containing components of very different solubilities: although the solvophobic polymer component segregates from the solvent, the other solvophilic polymer component can interact both with solvent (possible structures B2, b1, and b2 in Figure 1) and with the segregated solvophobic polymer part (possible structures b3/B3, b4/B4, and b5/B5 in Figure 1). By changing the viewpoint and considering the solvophobic component, there can be a competition between segregation and complexation at the same time: the solvophobic polymer either undergoes total segregation (toward solvent and solvophilic polymer; b1 and B2 in Figure 1) or it undergoes complexation with the solvophilic polymer. Under which circumstances does one interaction prevail? What will be the structure of the colloidal entities? Could there be any intermediate situation where both segregation and complexation are well balanced, and how would these micelles look? A possible answer to these questions is also shown in Figure 1b3/B3. Here, a micellar core−shell−corona structure made of simple diblock copolymers is postulated, but other morphologies and polymer architectures can be envisioned as well (e.g., worms/vesicles). They would further enrich the micellar variety. For instance, the balance of segregation and complexation could yield micellar multicompartment containers[52−56] with two different solvophobic domains only by the use of binary amphiphilic polymers. However, actual examples of such micellar constructs are rarely described. This might be due to a lack of profound knowledge of interaction patterns, which is required to proceed with advanced macromolecular and micellar engineering to such well-balanced/subtle structures. Furthermore, it is rather difficult to predict the morphology of the otherwise segregated micellar construct:[22] whereas the complexation-induced increase in solvophobic volume and the concomitant shift in solvophobic/solvophilic balance would favor wormlike and vesicular aggregates compared to spherical core/corona micelles (analogous to Israelachvili's packing parameter),[57] the possible complexation-induced reduction of interfacial tension between the insoluble components and solvent would hint at the opposite direction. Below, we will discuss a specific example in which the latter contribution is dominant for branched systems though segregation prevails for block copolymers.

After making the reader aware of possible extensions in the general micellization scheme, we will discuss specific examples in the following text. We will discuss the PPO and PDMAEMA couple and also the PNIPAM and PDEAAM couple and compare the experimental results with the results from optimized[58] Monte Carlo simulations.[59,60] We dedicate one section to highlighting the general behavior of PPO with respect to PDMAEMA before we discuss different measures to influence the PPO/PDMAEMA interaction. We know that architectural aspects have a direct influence on the polymer properties.[61] This also includes complexation. However, a full understanding of the underlying mechanisms with respect to architecture is missing. This review is supposed to contribute to this area, emphasizing compositional aspects (monomer sequence: statistical copolymers vs block copolymers) and topological aspects (stars vs linear polymers). Because investigating different interaction strengths gives a more broad understanding of the subject, we also regard different types of interaction. As an example, we pick systems governed by van der Waals interactions and hydrogen bonding. Then, the

DOI: 10.1021/acs.langmuir.6b04602
Langmuir 2017, 33, 4091−4106

requirements for harvesting weak effective attractions (e.g., for hydrogen bonding or van der Waals attraction) in dilute solution and at interfaces are discussed.[60]

IDENTIFYING COMPLEXING POLYMER COUPLES

To investigate the effect of complexation, one first needs to find polymers that form a complex. Theoretical approaches can help to find such suitable couples. However, the direct prediction and application of the Flory–Huggins interaction parameter, χ, for a certain polymer/solvent and polymer/polymer couple is sometimes difficult[62] because χ is altered by architecture.[63] From a practical point of view, other concepts apart from the Flory–Huggins theory were introduced to predict the polymer solubility. Hildebrand related the solvent/solvent interactions to the parameter δ, which is the square root of the vaporization enthalpy per molar volume.[64] The latter is proportional to the intermolecular attraction. Polymers and solvents with similar δ values are believed to have similar attractive forces, and solubility is predicted according to the principle "like dissolves like". To relate the solubility to functional groups with different types of interactions (such as dispersion forces, dipolar interactions, or H-bonding), Hansen introduced a three-dimensional space to categorize both solvents and polymers.[65] Again, the solubility is predicted for spatial proximity between the location of the polymer and solvent in Hansen space.

Atactic PPO is an oily, low-T_g viscous polymer, and the crystallization of PPO is favored when the isotactic content is increased, leading to solid materials with reduced solubility.[66] In contrast, atactic PPO of moderate molar mass is soluble in very different solvents such as (warm) hexane and (cold) water.[67] This behavior can be termed chameleonic,[68] increasing the expectation that compatibility between PPO and other polymers can be found.

Beneficially, atactic PPO is known to have a rather large interaction radius in Hansen space,[69] meaning that rather different solvents are good solvents for PPO and the number of nonsolvents is rather low.[70] There were attempts to predict such interpolymer complexation leading to (partial) miscibility with the aid of solubility parameters. By extrapolating literature data for the Hildebrandt parameter δ, one obtains $\delta \approx 17$ $(\mathrm{J\ cm^{-3}})^{0.5}$ for PDMAEMA at 25 °C.[71] In turn for PPO, the Hoy concept of calculating δ by regarding additive molar cohesion of all substituents and backbone components gives $\delta \approx 17$ $(\mathrm{J\ cm^{-3}})^{0.5}$.[72] This value is in accordance with experimental PPO literature data.[73] Hence, the theoretical Hildebrand approach points to a compatibility of the polyether PPO and the structurally rather different methacrylate-based PDMAEMA (Figure 2). Indeed, the bulk miscibility of PPO and PDMAEMA was demonstrated for their corresponding block copolymers,[26] indicating that both partners are prone to form polymer complexes under certain circumstances.

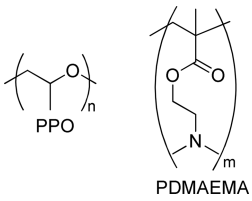

Figure 2. Structure of poly(propylene oxide) PPO and poly(dimethylaminoethyl methacrylate) PDMAEMA.

We also discuss the monomer sequence[61] within NIPAM and DEAAM copolymers (Figure 3), although the corresponding block copolymers have only a low tendency to segregate (within certain temperature/concentration regimes, they provide examples from the top rows of Figure 1: a2, a5, and a6/A6).[74] At the same time, we investigate their thermoresponsive properties. These properties are also a direct measure of the complexation between the NIPAM and DEAAM units. After discussing such NIPAM- and DEAAM-based copolymers, we will switch to another segregation strength when turning to the PPO/PDMAEMA couple (they provide examples from the bottom rows of Figure 1: B2, b3/b4).[47,75] In the following text, we place emphasis on our own work but also compare related work from other authors.

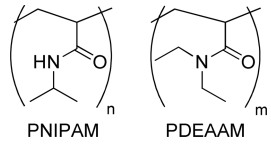

Figure 3. Structure of poly(*N*-isopropylacrylamide) PNIPAM and poly(*N*,*N*-diethyl acrylamide) PDEAAM.

MONOMER SEQUENCE: COPOLYMERS OF NIPAM AND DEAAM

Hydrogen bonding is an important parameter in many aqueous polymer solutions. Intrapolymeric H-bonding is often involved in LCST behavior[76] and UCST behavior.[77] As a consequence, the cloud point of PNIPAM can be reduced by offering a more efficient H-bond acceptor than PNIPAM itself.[78] An efficient H-bond acceptor requires an increased electron density, which can be provided at a PDEAAM carbonyl oxygen. Here, the two ethyl groups inductively donate electron density to the amide bond.[17] Different substitution patterns at the amide nitrogen of poly(acrylamides) can lead to quite different cloud points.[79] But even though PDEAAM lacks the polar secondary amide proton of PNIPAM and conveys an additional carbon atom per monomeric unit, both polymers phase separate close to 32 °C.[23] The reason for the almost identical LCST of PDEAAM and PNIPAM might be enhanced H-bonding, even to water. With this background, one would expect rather invariant cloud points upon copolymerizing acrylamides NIPAM and DEAAM, but a synergistic effect can be observed for copolymers of NIPAM and DEAM.[78]

In this context, the influence of the arrangement of segments along the polymer chain needs to be addressed. Is mere connectivity sufficient to trigger the synergistic behavior, or is spatial proximity required? A block copolymer would suffice for the connectivity criterion, whereas a statistical copolymer provides a close prearrangement of the interacting sites. Therefore, copolymers with similar molecular weight were prepared by controlled radical polymerization. At the same time, copolymers with a blocklike arrangement and statistical arrangement were compared to their homopolymers.[74]

The homopolymer mixtures were reported as being unaffected by the presence of the other partner, yielding phase-separation temperatures close to those of the pure homopolymers.[40] The block copolymers phase separate at temperatures that are close to those of the homopolymers, showing that mere connectivity is not sufficient to induce complexation. In contrast, statistical copolymers of PNIPAM

DOI: 10.1021/acs.langmuir.6b04602
Langmuir 2017, 33, 4091–4106

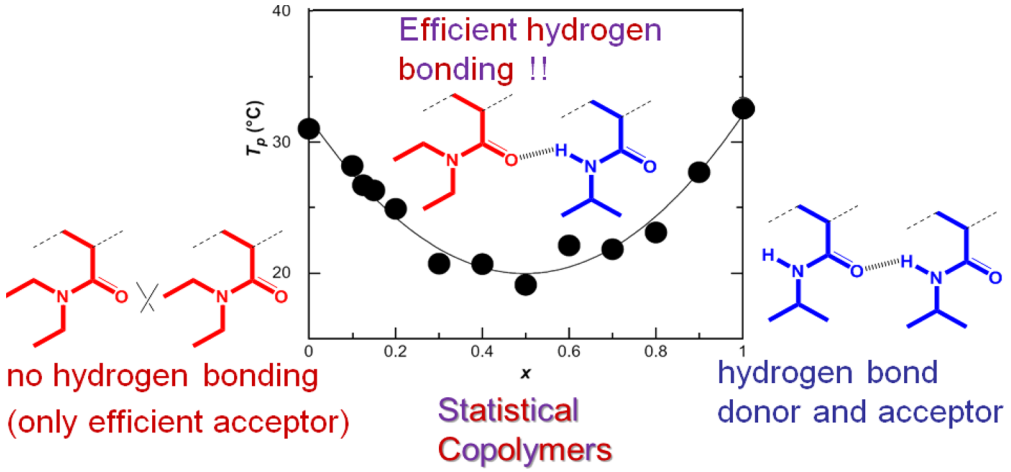

Figure 4. Typical phase diagram for copolymers of NIPAM and DEAAM as a function of the NIPAM mole fraction x (adapted from ref 40 with permission from Elsevier).

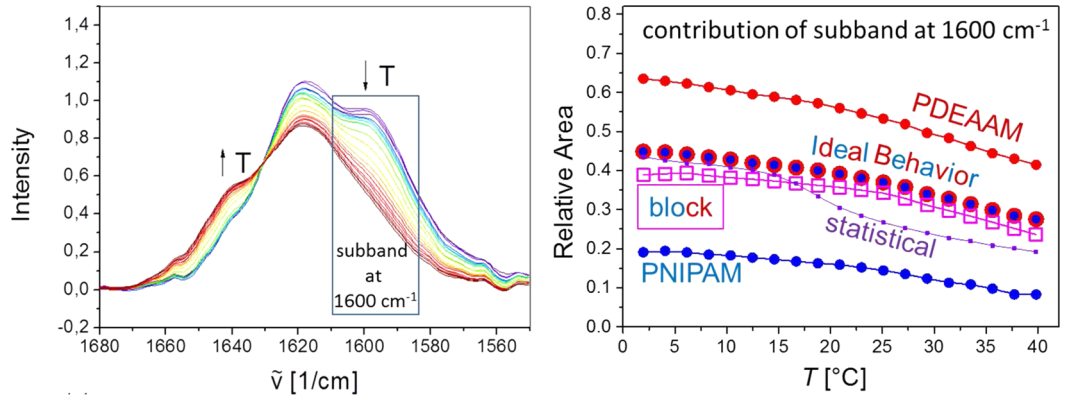

Figure 5. Temperature-dependent IR spectra of the amide I′ band of a statistical copolymer (left) and the temperature-dependent contribution of the subband at 1600 cm^{-1} for the homopolymers (red PDEAAM, blue PNIPAM), their theoretical arithmetic average (red dots with blue interior), the statistical copolymer (purple line), and the diblock copolymer (pink squares; adapted with permission from ref 74).

and PDEAM showed a pronounced synergistic depression of cloud points.[78] A 1:1 copolymer exhibits phase separation at 20 °C instead of the expected 32 °C (Figure 4). Naturally, preferred hydrogen bonding between the two interacting species is proposed as an explanation for attraction between the species, leading to complexation.[80] This indicates that connectivity as such is not the only reason for the depression of the cloud points.

It turns out that the block copolymers behave like an ideal mixture of homopolymers. This is seen by IR analysis of the temperature-dependent amide I′ band (Figure 5, left side), which can be divided into subbands. For the block copolymer, the subband fractions resemble the arithmetic average of the PDEAAM and PNIPAM homopolymer fractions. By this calculation, each homopolymer contributes to the subband according to the composition of the copolymers when possible synergistic effects are absent. Hence, the block copolymer shows the behavior of the ideal PDEAAM and PNIPAM mixture, and the statistical copolymer deviates from the ideal curves.

There is no direct evidence for a zipping mechanism between the different blocks (structures A2 and A5 in Figure 1). The rather weak interaction between NIPAM and DEAAM does not pay for the loss in conformational entropy upon intramolecular folding of the NIPAM-based block to the PDEAAM block. In contrast, the spatial proximity between DEAAM and NIPAM units within the statistical copolymer provides a good condition for enhanced interaction. These observations and interpretations indicate that the local (mutual) concentration between weakly interacting partners is essential for the interaction.

In sum, these experiments show that the preferential interaction between NIPAM and DEAAM units can be best harvested in a statistical copolymer. A strictly alternating polymer of DEAAM and NIPAM is hardly accessible; one might expect that the alternating sequence could even prevail over the performance of the statistical one. In contrast, the block copolymer prevents the synergistic interaction between the two constituents.

By simulating a simple coarse-grained model consisting of a generic polymer made up of A and B beads, which attract each other, we were able to obtain deeper insight into the aforementioned system.[59] Comparing the properties of an alternating (as an approximation for a statistical copolymer) and a diblock copolymer gives insight into the processes involved in the complexation of the DEAAM/NIPAM polymers. These simulations show that within an alternating copolymer the collapse of the polymer is visible at very small attractive interaction potentials (Figure 6). In contrast, the diblock copolymer is unaffected until a considerably larger interaction potential is applied. Above a certain threshold (~0.5

DOI: 10.1021/acs.langmuir.6b04602
Langmuir 2017, 33, 4091−4106

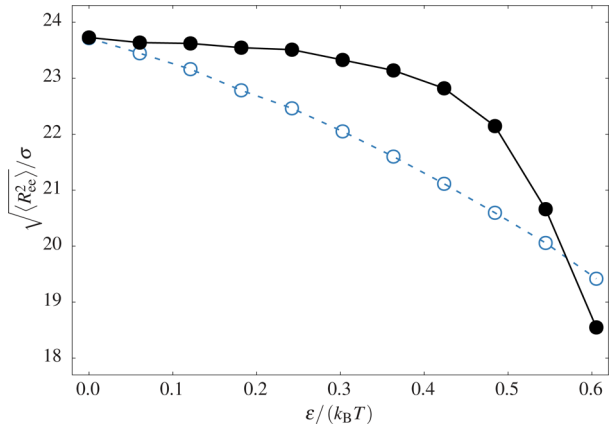

Figure 6. End-to-end distance in units of the bead diameter σ of a terminal 100-bead section as a function of the interaction parameter ε for 1:1 diblock copolymers (black filled symbols; each block is 100 beads long) and for strictly alternating copolymers with an A/B ratio of 1:1 (blue open symbols; total length 200 beads; adapted in part from ref 59 with permission from Wiley).

k_BT), the diblock copolymer is even more effective in arranging an internal complexation than the alternating copolymer. This can be explained by the many mutual contacts available upon looping back. Despite the spatial proximity of comonomers in an alternating copolymer, a large number of mutual contacts are already prearranged along the chain. These next-neighbor contacts, however, do not increase the number of newly arranged, attractive contacts, which would have been expected upon conformational reorganization. Because of complexation, this precollapsed state of the alternating copolymer makes the transition to an insoluble collapsed structure more favorable. This explains the experimental results for the statistical copolymers.

We conclude that statistical copolymers are capable of harvesting weak interactions, whereas the complexation is even more pronounced for diblock copolymers at intermediate interaction energies (we define the border between strong and weak interaction at ~1 k_BT; ionic interactions can be more than 1 k_BT). These observations are in line with the experimental results. By the aid of the transition-temperature decrease, a destabilization of the soluble structure of the statistical copolymer compared to that of the block copolymer can be estimated to be on the order of 0.03 k_BT. In the statistical copolymers, the weak attraction between DEAAM and NIPAM is sufficient to render such a destabilization, whereas the block copolymers are not suited for harvesting the synergistic behavior.

POLYMER TOPOLOGY: COPOLYMERS OF PPO AND PDMAEMA

We have already learned that statistical/alternating copolymers are efficient in harvesting very weak mutual attractions between the different monomeric units. This was shown for DEAAM- and NIPAM-based copolymers. To enhance the effect of segregation, we turn to the PPO/PDMAEMA couple, where PPO forms hydrophobic aggregates in the heat. However, statistical or even alternating copolymers of propylene oxide PO and dimethylaminoethyl methacrylate DMAEMA are not available with the current synthesis toolbox. Only blocklike polymers, which are also favorable for efficient segregation, are available. Hence, measures other than statistical copolymers need to be taken in order to harvest the effects of the weak attractive forces between PO and DMAEMA units. One of the successful measures is the introduction of a branched architecture.[81] Hence, the solution properties of a star-shaped copolymer[82] were compared with those of the corresponding diblock copolymers in order to study the effect of topology. So-called miktoarm stars are compared to related combinations such as PPO-*b*-PDMAEMA and PPO-*b*-PEO with similar block lengths as in the miktoarm star.[75] Miktoarm stars are star-shaped polymers where different polymeric constituents are linked by one central core.[83]

Interestingly, hardly any attention was paid to the PPO/PDMAEMA interaction until 2011, when their bulk miscibility was discovered.[26] Though studies of PPO- and PDMAEMA-containing systems in dilute aqueous environments are available, none of them mention any preferential interaction between both partners.[84,85] Hence, special requirements are needed to induce a complexation between PPO and PDMAEMA in dilute media. This is due to a rather weak attractive interaction. Then, advanced macromolecular architecture is essential to harvest this interaction in dilute aqueous solution. Hence, architectural effects on polymer−polymer complexation are one important aspect in this review as we try to answer the question of whether PPO segregation or PPO/PDMAEMA complexation prevails in PPO- and PDMAEMA-derived copolymers. Here, the three-dimensional connectivity of the chains comes into play by addressing the topology of polymers at the same time.[86] Note that the introduction of branching (as achieved by taking star-shaped, brush-shaped, or hyperbranched/dendritic polymers) also increases the number of end groups, which might affect T_g and the overall solubility of the macromolecular construct.[87]

For PPO/PDMAEMA, the exact origin of complexation is still under debate. We assume that rather short-ranged van der Waals forces (such as dipolar interactions) are important. Amplified by crystallization, these van der Waals forces are often the reason for the interaction between polymers of different tacticity, leading to stereocomplex formation. Syndiotactic and isotactic polymers precipitate simultaneously from a common solution, as is known for PMMA[48] and poly(L-lactide)/poly(D-lactide).[49] Stereocomplex formation between chemically different polymers is rather rare.[88] In this case, they form so-called heterostereocomplexes. A similar mechanism cannot be excluded for the complexation of atactic PPO with atactic PDMAEMA on a more local level. Then, the attraction of certain triads in the PDMAEMA backbone (such as *mr* triads) to a certain configuration or conformation of PPO might facilitate the interaction, as indicated by NMR.[47,75] In turn, the solubilizing noncomplexing dimethylaminoethyl groups of PDMAEMA are still available to provide colloidal stability,[25] which also explains the low interfacial tension of the PPO/PDMAEMA complex toward water.[47]

The evolution of hydrophobic domains with temperature was investigated for all polymers. PPO is a thermoresponsive polymer with a rather low transition temperature,[23] and PDMAEMA has higher transition temperatures, dependent on pH (here close to 55 °C).[89] At low temperature, all of the involved polymers are supposed to be well solvated and soluble. Then upon heating, PPO is expected to become insoluble first.

We trace the evolution of the hydrophobic domains with suitable probes, such as pyrene and 4-(dicyanomethylene)-2-methyl-6-(4-dimethylaminostyryl)-4*H*-pyran (4HP). Pyrene is a well-known fluorescent probe for the detection of hydro-

DOI: 10.1021/acs.langmuir.6b04602
Langmuir 2017, 33, 4091−4106

phobic surroundings. The intensity of vibrational subbands I_1 and I_3 is affected by the surrounding polarity (leading to changes in I_3/I_1). 4HP detects a hydrophobic environment by a virtual shifting of the emission peak (by different contributions of two overlapping, broad emission peaks).[90] A nonpolar environment causes a decreasing wavelength λ_{max} at the maximum in the emission spectrum. By taking λ_{max}, the formation of hydrophobic domains (as in the form of micelles) can be traced (Figure 7). Each dye has advantages and

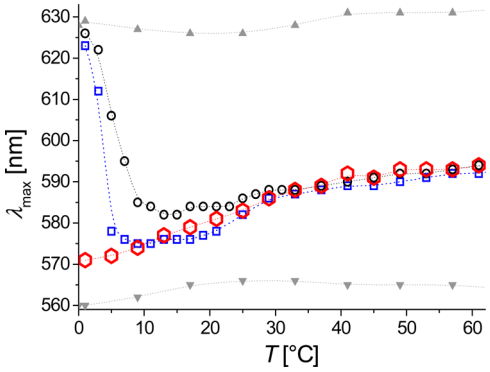

Figure 7. Fluorescence spectroscopy of different polymer solutions in pH 8 buffer (+ 0.1 M NaCl) showing the wavelength at the emission maximum λ_{max} of 4HP as the probe (10^{-6} M; λ_{exit} = 470 nm, λ_{em} = 480−750 nm); assignment: 1.0 g/L PEO_{114}-$(PDMAEMA_{90})_{3.1}$-PPO_{69} miktoarm star polymer (red, open hexagons; indices assign the degree of polymerization and the arm number respectively), 0.4 g/L PPO_{69}-*b*-$PDMAEMA_{100}$ (blue, open squares), 0.16 g/L PEO_{114}-*b*-PPO_{69} (black, open circles), and for comparison pure PPO_{69} (without solvent; downward-directed gray triangles) and pure solvent (without polymer; upward-directed gray triangles; for all, heating 20 K/h; lines are a guide to the eye; reprinted with permission from ref 47).

disadvantages. For example, 4HP is more insensitive to fluorescence quenching because of the presence of tertiary amine groups, which can be an issue for pyrene. In turn, pyrene gives a more gradual response due to gradual changes in the intensity of the subbands, whereas λ_{max} of 4HP could provide a more stepwise transition (on−off/digital) due to the dominion of one of the subbands. In the following text, we concentrate on 4HP measurements and a qualitative picture, whereas later a quantitative comparison with simulations is based on the analysis of the pyrene response.

For both block copolymers PPO-*b*-PEO and PPO-*b*-PDMAEMA, λ_{max} is close to the value of 4HP in pure solvent at temperatures of around 0 °C, meaning that both the fluorescent dye and polymer are well solvated. λ_{max} drops above 5 °C, which indicates the evolution of the first hydrophobic domains. This could be caused by assembled polymer (micelles) or even by unimolecular micelles, which consist only of one polymer, hosting a shielded hydrophobic domain. Finally, λ_{max} levels off at approximately 15 °C.

The behavior of miktoarm star PEO-$(PDMAEMA)_{3.1}$-PPO is different (the PEO arm is noncomplexing but acts as a reference for all experiments; see also below).[47] The single constituents are soluble at low temperature, and the star-polymer solution exhibits nonpolar, hardly solvated domains at these temperatures. This is demonstrated by a rather low λ_{max} value at 1 °C. This unexpected behavior can be traced back by different techniques. IR spectroscopy of the carbonyl stretching vibration shows features of a nonpolar environment at low temperature.[75] The PDMAEMA groups are apparently involved in some type of complexation. NMR showed a decreased intensity of both PPO and PDMAEMA signals in the star polymer (compared to the unaffected PEO signal), which is in favor of complex formation between PPO and PDMAEMA. Most striking is probably the analysis of the fluorescence data (Figure 7), whose λ_{max} can be interpreted as the arithmetic average over the signal of entrapped dye and the signal of dye dissolved in the bulk solution. Upon heating, the partitioning changes according to the involved thermodynamics. The equilibrium constant for dye uptake into the hydrophobic domain can be extracted, and with such temperature-dependent data at hand, the entropy and enthalpy of dye uptake can be derived by the help of the van't Hoff equation.[91] Then it turns out that the thermodynamic parameters for dye uptake are identical for both the PEO-*b*-PPO micelles and the PPO-*b*-PDMAEMA micelles. That means that in both cases the chemical environments in the micelle interiors are the same. They possess a PPO-dominated core, and hence PPO segregation prevailed for the micellar PPO-*b*-PDMAEMA/water system (structure B2 in Figure 1). Still, we are rather close to a balance of segregation/complexation, which is seen in the following fact: in contrast to the diblock copolymers, the miktoarm star does not provide a pure PPO domain but a different microenvironment in aqueous solution. This can be explained by the presence of a complex, altering the polarity of PPO by mixing with PDMAEMA (equivalent to structures B4 and B5 in Figure 1).

These results show that the local segment density is again essential for the effectiveness of complexation (or the effectiveness of a weakly attractive pair potential). The loss in conformational entropy does not allow an efficient folding of one block to the other block in the case of weak attraction between the different parts in block copolymers. However, hardly any back bending is required for the different arms in the miktoarm star, as the interacting sites are close anyway (especially at the core of the star). The increased mutual segment density within the miktoarm star enhances the complexation. By analogy, polymers with PPO grafts along a PDMAEMA backbone might also lead to complex formation:[92] a comparison of the NMR in good (chloroform) and selective solvent (D_2O) shows a considerable reduction in the signal for PDMAEMA in comparison to PPO when changing the solvation from organic to aqueous solution. This is despite the fact that PDMAEMA should be soluble and PPO should be insoluble under the conditions used.

Simulations allowed us to rationalize these results on miktoarm stars and diblock copolymers. We saw before that an alternating arrangement renders an enhanced interaction between the attractive partners at low interaction energies. Similarly, the miktoarm stars enhance the complexation compared to that of the corresponding diblock copolymers (Figure 8). In the model, one arm (B, in our context PPO) is kept the same throughout all simulations. For the other arm type (A, in our context PDMAEMA), the length (in the case of the diblocks) or the number of arms (in the case of stars) is varied. The behavior of the B arm was investigated by comparing miktoarm stars to diblock copolymers with the same molecular weight and composition. Upon increasing the arm number at very low attractive interaction energies ε, there is an increase in the end-to-end distances of both A and B arms compared to the situation in the diblock. This is a direct consequence of excluded volume effects. However, upon

DOI: 10.1021/acs.langmuir.6b04602
Langmuir 2017, 33, 4091−4106

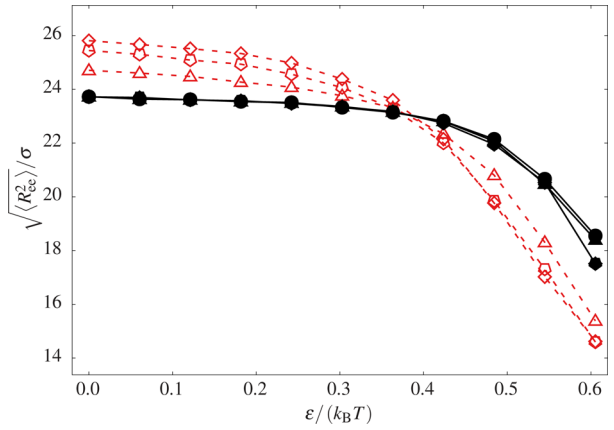

Figure 8. End-to-end distance of the polymer arms as a function of the interaction parameter ε for star polymers with 1 (black circles), 3 (red open triangles), 5 (red open pentagons), and 7 (red open diamonds) A arms (all arms for stars: N = 100 beads each) and end-to-end distance for diblock copolymers with N = 100 (black circles; in total 200 beads), N = 300 (black filled triangles), N = 500 (black filled pentagons), and N = 700 (black filled diamonds) A particles. Most symbols for the diblock copolymers overlap. (Adapted in part from ref 59 with permission from Wiley.)

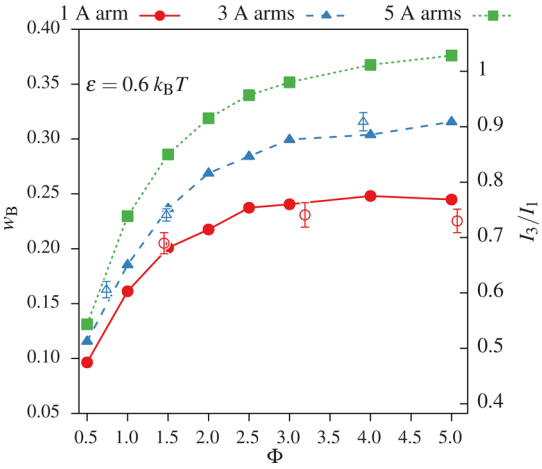

Figure 9. Comparison of the simulated fraction of complexed B particles (~PPO beads in the complex) at ε = 0.6 k_BT (full symbols, left axis) to the experimentally measured hydrophobicity (I_3/I_1 at 1 °C, open symbols, right axis; reproduced with permission from ref 93.)

increasing the strength of the attraction between A and B beads, the collapse of the B arm in the miktoarm star is more pronounced than the collapse of the B block in the diblock copolymer. For the block copolymers, the collapse of the B arm is hardly affected by any excess length of the A arm (the diblock copolymers show all the same behavior for the B arm), but the increase in the arm number strongly affects the conformation of the B arm. This is a direct indication of the enhanced complexation between A and B in the miktoarm star.

By systematically varying the composition and the topology in both the experiment and the simulations, we gained better insight into the internal complexation behavior. The content of PDMAEMA (A beads) was changed within one type of topology, whereas the topology was changed at constant composition. Hence, diblock copolymers and miktoarm star polymers with different arm numbers and block lengths were investigated. To further improve the comparability between both methods, we performed fluorescence experiments with pyrene as a probe molecule, which is able to reflect more gradual changes in the complexation behavior.[93]

The fraction of complexed PPO was extracted from the simulations. Most strikingly, the experimental I_3/I_1 ratio at low temperatures shows the same relative trends as the fraction of complexed B beads in the simulations (Figure 9). Hence, the fraction of complex from the simulations correlates to the pyrene fluorescence response of these polymer solutions. As another important finding, we see now limited complex formation for the diblock copolymers, which seems to contradict the 4HP results. Therefore, it is reasonable to assume that the 4HP method underestimates the complexation in the case of diblock copolymers. Here, the pyrene method gives larger values for the content of the complex (or the content of complexed PPO), which are well in line with the simulation results. Nevertheless, the 4HP results nicely reflect the general trends, which were also corroborated by the pyrene method and the simulations: higher branching and a higher content of PDMAEMA (A beads) favor complexation and lead to an increased amount of PPO (B beads) in the complex.

Such enhanced complexation (in the miktoarm star) can have far-reaching (and amplified) effects, as will be discussed in the following text for the structure of these hydrophobic entities (micelles). After having learned about the special interaction of PDMAEMA and PPO within these polymers, the aggregation behavior with temperature needs to be addressed. This question was answered using scattering methods, mainly with a combined dynamic light scattering (DLS) and static light scattering (SLS) approach but also with small-angle X-ray scattering (SAXS). The DLS and SLS combination allowed not only the extraction of the different hydrodynamic radii for a complex multicomponent system but also the extraction of the amount of scattered light originated from each scattering entity.

Under certain conditions, one would expect the coexistence of unimers and micelles. This is also true for our system, but so-called loose aggregates in the size range of 100 nm are also detected. Their overall contribution is small, though the amount of light they scatter can be considerable because of their large size and molar mass. Such loose aggregates were often observed for water-soluble polymers, and their origin is still under debate.[94,95] By the help of this combined DLS and SLS attempt, we were able to extract the scattering intensity of the unimers and micelles alone or in combination with the loose aggregates, whose reorganization can be followed by the same method (Figure 10). This was achieved by extrapolating to low angle for each temperature. The obtained extrapolated scattering intensity (as red bars) for each species correlates directly to the product of mass concentration and molar mass (according to the Zimm equation).[96] By certain assumptions, it can be translated into a mass contribution (blue bars in Figure 10). Generally, scattering from unimers (hydrodynamic radius $R_h \approx 5$ nm) can be seen up to approximately 20 °C for a PEO-*b*-PPO solution.[75] At higher temperatures, the unimers aggregate into micelles (their scattering increases), and the scattering of the loose aggregates decreases. In contrast, unimers are detected up to high temperature for the miktoarm star, though the polymer contains hydrophobic domains even at very low temperature (Figure 7). It turned out that approximately 99% of the miktoarm stars are present as unimers (even up to 49 °C). This result was corroborated by an independent determination of the average aggregation number N_{agg} using a fluorescence quenching approach.[97] Hence, it is

DOI: 10.1021/acs.langmuir.6b04602
Langmuir 2017, 33, 4091−4106

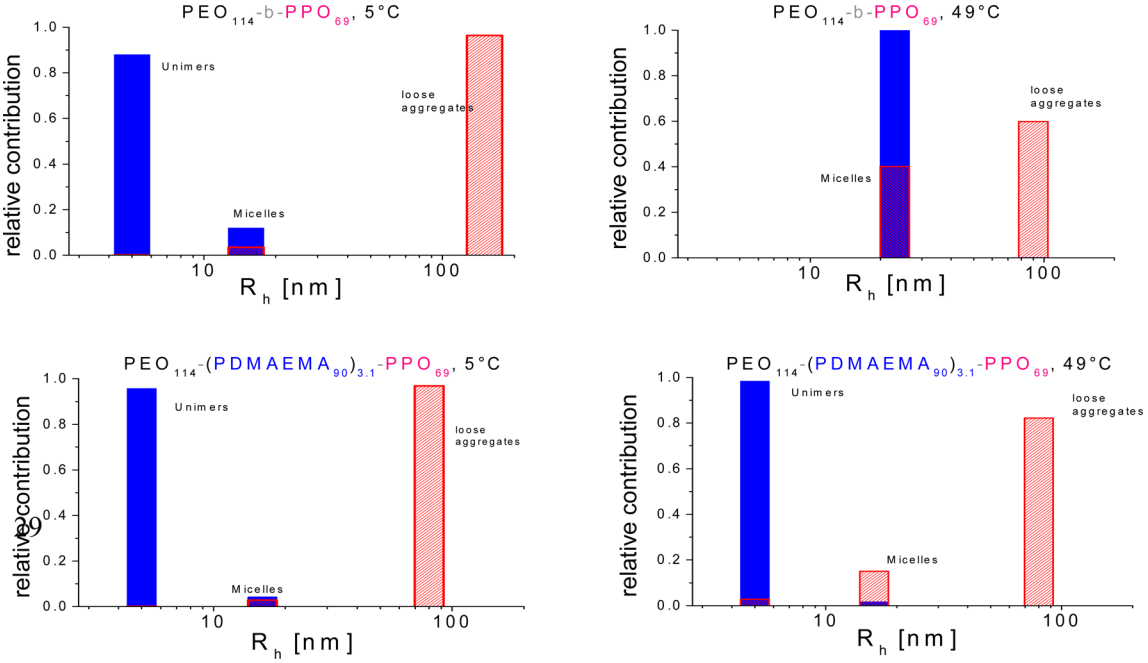

Figure 10. Comparison of the intensity of scattered light (extrapolated to $q \rightarrow 0$; red, open striped bars) with the mass concentration by use of a scaling approach (blue full bars); the left diagrams are at 5 °C, and the right-hand side is obtained at 49 °C. Top row: PEO_{114}-*b*-PPO_{69}. Bottom row: PEO_{114}-$(PDMAEMA_{90})_{3.1}$-PPO_{69} (adapted from refs 47 and 75 with permission from the American Chemical Society and the PCCP Owner Societies, respectively).

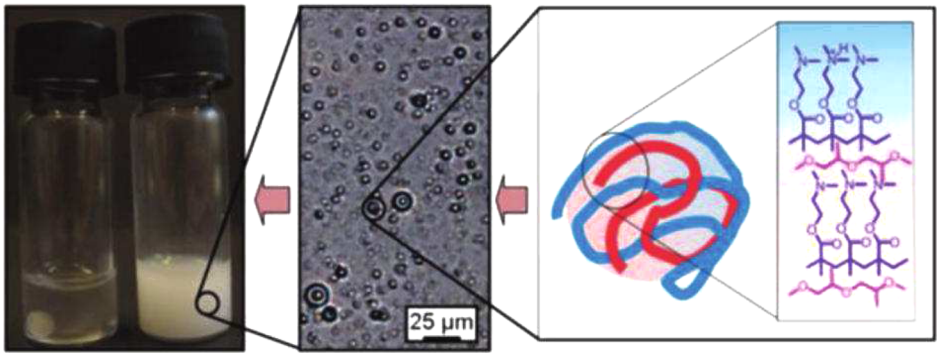

Figure 11. PDMAEMA acting as a complexant and as a microsurfactant (right-hand side), leading to a colloidal stabilization of PPO in the aqueous phase (images; left vial, 5 wt % PPO in water; right vial, additional 5 wt % linear PDMAEMA; optical micrograph of the same dispersion; all images taken at room temperature; reproduced from ref 47, copyright 2012 American Chemical Society).

quite surprising that the PEO-*b*-PPO aggregates into micelles with an approximate N_{agg} of 200 (as assessed by SAXS), whereas the introduction of three more soluble arms reduces N_{agg} to unity. Another scaling approach helps us to understand this observation.

We need to address the influence of a varying arm number on N_{agg}, when the arm number of the soluble component is changed (here, differences in PDMAEMA and PEO are neglected because of their similar arm lengths). One would expect a decrease in the aggregation number by increasing the number k of soluble grafts due to increasing spatial demands of the soluble component. This can be quantified theoretically by a scaling approach ($N_{agg} \approx k^{-3/5}$) when assuming the presence of spherical (core−corona-type) micelles (as observed in our system).[47] Then, the aggregation number should drop from about 200 to approximately 90 when increasing the arm number k from 1 to 4. Hence, the spatial demands inside the corona of the proposed miktoarm star micelles cannot explain the drastic reduction in N_{agg}. This corona effect is even less pronounced when assuming complexation. The only parameter that enters the scaling and can explain the drastic reduction in aggregation number is the interfacial tension between the complex and bulk water. And indeed, experiments at higher concentrations of both homopolymers revealed the beneficial role of PDMAEMA, covering the complex and reducing its surface tension considerably. Because PDMAEMA is more soluble than PPO, it stays at the surface of the complex and acts like a microsurfactant (possible structures b2, b3, and b4/B4 in Figure 1; see also Figure 11). Therefore, the soluble component transfers its solubility to the complex, which becomes well dispersed. Here, major aggregation is prevented and colloidal stability is provided. Hence, we conclude that the complexation between an insoluble and soluble homopolymer in most cases increases the colloidal stability of stoichiometric complexes, whereas the complexation between equally soluble polymers in

DOI: 10.1021/acs.langmuir.6b04602
Langmuir 2017, 33, 4091−4106

a stoichiometric ratio often decreases the colloidal stability (as seen for NIPAM/DEAAM-containing copolymers).[74]

We also conclude that the starlike architecture promotes induced, internal complex formation (analogous to structure B4 in Figure 1), which overcomes the tendency to segregate, which is otherwise encountered in the PPO-containing block copolymers (B2): both PPO-*b*-PDMAEMA and PEO-*b*-PPO form micelles with PPO in the core without any indications of complex formation at high temperature. However, the fluorescence data shows a slightly more hydrophobic complex on the edge of PPO insolubility at low temperatures before segregation and micellization occur.

There are also some indications that segregation prevails for complexes of other PPO-containing complexes such as block copolymers of PPO and PAA,[98] which can undergo hydrogen bonding. For PAA-*b*-PPO-*b*-PAA, a reentrant transition was reported upon heating. The solutions become turbid (probably at the beginning of the PPO transition, also inducing the complexation between PPO and PAA at low pH), and further heating leads to clear solutions, which could be micellar constructs with PPO in the core.[98] Hence, these polymers could behave analogously to PPO-*b*-PDMAEMA, with the difference being that no pronounced turbidity is visible for PPO-*b*-PDMAEMA below the transition of PDMAEMA. This might be caused by the stronger hydrogen bonding between PPO and PAA compared to the interactions of PPO and PDMAEMA. Referring to Figure 1, we therefore postulate a reversed sequence for PAA-*b*-PPO-*b*-PAA: the block copolymer intermingles upon initial heating (analogous to structure B5 in Figure 1) before it rearranges into core−corona micelles (B2 or even B3/B4). For the PPO-*b*-PDMAEMA diblock copolymer, the schematic description in Figure 1 ends after the formation of the core−corona star-shaped micelle (structure B2 in Figure 1). This behavior is in contrast to the miktoarm star, which prevents this core−corona star-shaped micellar structure but moves immediately forward to a structure analogous to B4 in Figure 1. This happens even without intermolecular aggregation. This is because the complexation enables a reduction of interfacial tension and finally leads to the prevention of aggregation. In this respect, the observed behavior is unprecedented: whereas complexation leads to aggregation for soluble homopolymers, the principles observed here prevent polymer aggregation in the case of amphiphilic systems. This behavior is summarized in Figure 12: changes in architecture (e.g., when going from a linear to a branched structure) can lead to completely different solution behavior. However, these observations are not general, as complex formation for PAA-*b*-PPO-*b*-PAA (induced by the stronger hydrogen bonding between PAA and PPO, which probably also allows back bending) leads initially to turbid solutions. Still, all of these observation provide confidence that micellar core−shell−corona structures of binary polymers (Figure 1, B3) might be available by fine tuning the system.

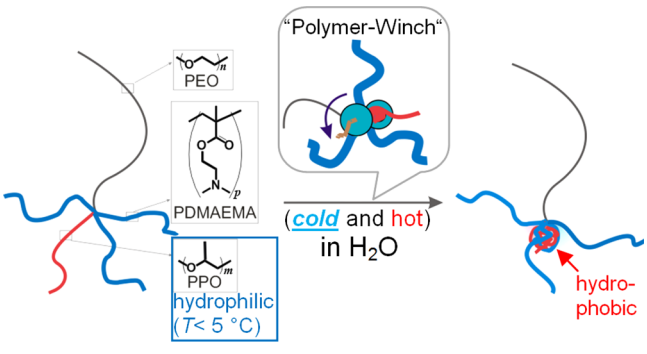

Figure 12. Internal complexation induces hydrophobicity but prevents intermolecular aggregation (interfacial tension reduction, reprinted with permission from ref 47, copyright 2012 American Chemical Society).

INTERFACIAL COMPLEXATION

By discussing three architectural possibilities (statistical, blocklike, and miktoarm star copolymers), it became clear that block copolymers are not predestined to efficiently harvest the complexation between weakly attractive monomers in dilute solution. At higher concentration or especially in the bulk, there are fewer architectural demands for the induction of complexation.[26,47] Therefore, we turned to other means of increasing the spatial proximity of both complexing blocks. One possibility would be to confine the polymer spatially, which could increase the proximity between all components of the polymer. One possibility of confining the polymer spatially is by bringing it onto an interface, which reduces the spatial freedom perpendicular to the interface: the polymer is confined in a slitlike (pseudo-) 2D space. It was investigated whether interfaces are capable of inducing an approach of the otherwise (entropically) avoiding blocks by comparing the compression (and expansion) isotherms obtained using a Langmuir trough. Compression isotherms give information on the spatial demands of the spread molecules at the interface and the ability to stabilize the interface. Here, the behavior of PPO-*b*-PEO, PPO-*b*-PDMAEMA, and PEO-*b*-PDMAEMA at an oil−water interface was investigated at 35 °C. In all cases, the block lengths were comparable. PPO is soluble in decane (and insoluble in water under the conditions used), whereas PEO and PDMAEMA possess an opposite solubility profile. Surprisingly, only PPO-*b*-PEO is a strong amphiphile, effectively stabilizing the interface down to rather low mean molecular areas, mma's. At the same time, rather high surface pressures SP can be achieved before film collapse occurs (Figure 13). In contrast, PPO-*b*-PDMAEMA is only weakly anchored at the interface, showing the expulsion of molecules from the interface upon compression at considerable lower SP than those for PPO-*b*-PEO (structures D in Figure 13). Such expulsion occurs at SPs comparable to those of bishydrophilic PEO-*b*-PDMAEMA, though PPO-*b*-PDMAEMA is supposed to be an amphiphile. Apparently, the amphiphilic behavior is weakened, probably similarly to what was observed for the reduction in interfacial tension upon complexation of PPO and PDMAEMA.[47] Even more surprising in the expanded state (structures A in Figure 13), PPO-*b*-PDMAEMA occupies a reduced interfacial area in comparison to PEO-*b*-PDMAEMA. All of these observations are in favor of a complexation of PPO and PDMAEMA in the diblock copolymer induced by the presence of the interface.

Why does the interface induce complexation between PPO and PDMAEMA? The surface energy of a clean decane/water interface is high, and the spread polymer (even the non-amphiphilic homopolymer) remains at the interface at low surface coverage (in the form of a so-called pancake-like conformation). This allows favorable contacts between the monomeric units of the polymer and the interface. Here, the less-polar moieties of a monomeric unit are located more in the oil phase, whereas the more-polar parts are directed toward the

DOI: 10.1021/acs.langmuir.6b04602
Langmuir 2017, 33, 4091−4106

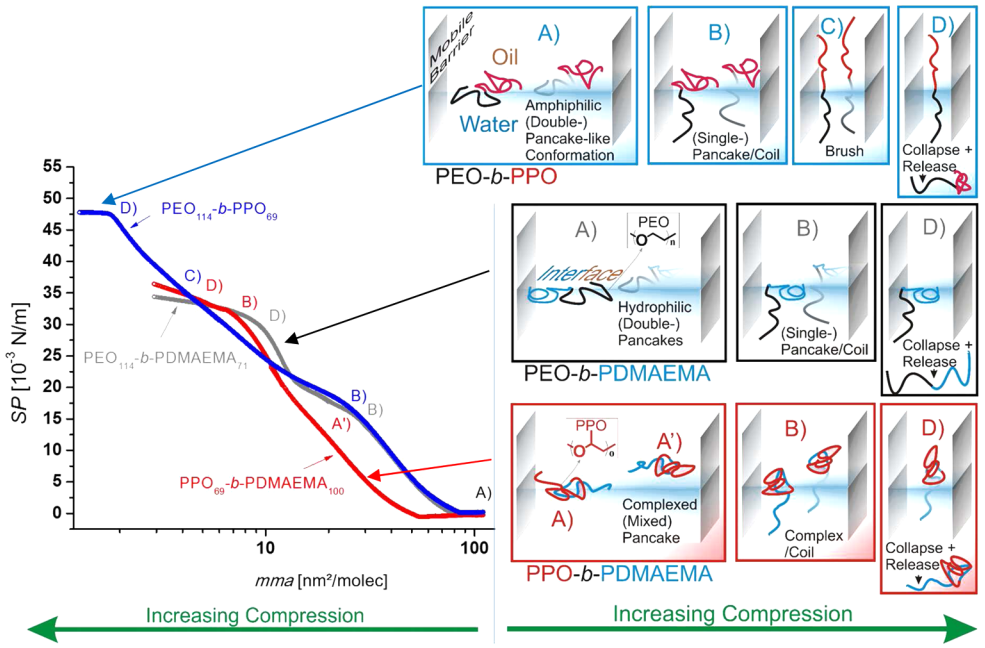

Figure 13. Compression isotherms of (block) copolymers PEO_{114}-*b*-PPO_{69} (in blue), PPO_{69}-*b*-$PDMAEMA_{100}$ (in red), and PEO_{114}-*b*-$PDMAEMA_{71}$ (in gray) at an *n*-decane−water interface at 35 °C: surface pressure SP against mean molecular area mma and a schematic molecular description of the isotherm features (here, the single PEO blocks are depicted in black; the PPO, in red; and the PDMAEMA, in blue; adapted from ref 60 with the permission of The Royal Society of Chemistry).

aqueous phase. Especially at high mma's, the polymer chains are rather confined to the 2D interface by their contribution to decrease the in interfacial tension; concomitantly, their conformational freedom is reduced considerably. As a consequence, the monomeric units of different blocks are now closer to each other than compared to the same polymer within a common solvent. This allows the harvesting of the weak attractive forces between the PPO and PDMAEMA blocks, leading also to a more compact sandwich-like pancake at the interface. Apparently, the presence of oil does not strongly influence the complexing abilities between PPO and PDMAEMA. In contrast, PPO-*b*-PEO and PEO-*b*-PDMAEMA try to maximize the covered surface per molecule, avoiding the sandwich structure in the expanded state. These observations are again in line with simulation results.[60]

In sum, the experiments probably provide the first report on the complexation of weakly interacting partners induced by a liquid/liquid interface. Instead of enhancing the solubilization of each complexant and thereby reducing the possible complex formation by offering good solvents for each complexant (a polar aqueous solvent for the hydrophilic PDMAEMA component and a nonpolar solvent for the lipophilic PPO component), the opposite is observed: complexation is facilitated in the pseudo-2D environment of a liquid/liquid interface. On the first level of understanding, this can be explained by the confining effect of such a (dilute) 2D environment, as the interacting partner is brought into closer contact compared to the situation in bulk solution.

CONCLUSIONS

As an important aspect of this review, different architectural pathways for the interaction enhancement between attractive comonomers were described. The statistical or alternating copolymerization is suitable for the weakest attractive interaction between the two comonomers. This was demonstrated for copolymers of *N*-isopropylacrylamide (NIPAM) and *N*,*N*-diethyl acrylamide (DEAAM). Their respective block copolymers do not give any indication of attraction between DEAAM and NIPAM, whereas the proximity of DEAAM and NIPAM and the concomitant induction of complexation in statistical copolymers leads to a detectable depression of cloud points in dilute solution. As an alternative, the (mutual) local segment density can be increased by use of miktoarm stars. At the core of the star, the availability of weakly attractive comonomers is increased considerably, without the need to pay a conformational (entropical) penalty as in diblock copolymers. Then the complexation inside the miktoarm star is facilitated, whereas the (pairwise) interaction potential needs to be increased in order to see a similar effect for block copolymers. However, the complexation can also be triggered by the preassembly of the block copolymers at liquid/liquid interfaces, whereas hardly any complexation takes place in bulk water. This was shown for copolymers made of dimethylaminoethyl methacrylate (DMAEMA) and propylene oxide (PO). In the absence of solubilizing, noninteracting parts, the complexation between equally soluble polymer constituents often leads to complexes of low solubility/colloidal stability. In contrast, the complexation of a soluble component with an already insoluble polymer (which might need some time for equilibration) can lead to complexes with increased colloidal stability or even to soluble internal complexes carried by single polymer molecules.

In conclusion, the miktoarm architecture is best suited for moderate interaction energies (as for PPO and PDMAEMA), and the statistical/alternating monomer sequence is preferred for weaker attraction (as observed for PDEAAM and PNIPAM). Taking the competition of segregation and complexation into account, researchers started to slowly approach this topic, especially when a delicate and subtle balance as a function of block length and pH influences the

DOI: 10.1021/acs.langmuir.6b04602
Langmuir 2017, 33, 4091−4106

complexed or segregated state of PDMAEMA-based block copolymers in heat (together with PAA).[99]

We hope that all of these results will stimulate more research in this area because other macromolecular architectures such as graft and hyperbranched polymers could provide proximity between weakly interacting partners in the dilute solution. Further advances are expected because other available materials (such as copolymer microgels with blocklike chains between cross-links)[100] might be predestined to show unexpected effects. Also, many more polymer couples with weakly attractive interactions are to be discovered. In this way, a better understanding of the structure−property relationship of such opposing effects of complexation on the interfacial tension and on the hydrophobic/hydrophilic balance would be helpful. We assume that simulation efforts could contribute significantly to advance this area of research. Then, the classical micellization scheme could be tremendously expanded, yielding new self-assembled entities with novel structures and properties. Those could help to fine tune the swelling or guest release profiles due to the complex-induced multicompartmental structures. Here, a fine tuning of the interaction strength would be beneficial, which might lead in the end to reversible switching between segregation and complexation. Finally, the unprecedented structures could also be preserved with the help of sophisticated cross-linking chemistry. We hope that this research opens a toolbox suitable for the precise engineering of interaction patterns and novel macromolecular structures. Then, we expect new applications to be at hand in a short time.

AUTHOR INFORMATION

Corresponding Author

*E-mail: plamper@pc.rwth-aachen.de.

ORCID

Pascal Hebbeker: 0000-0003-0754-103X

Felix A. Plamper: 0000-0002-0762-6095

Funding

German Research Foundation (Deutsche Forschungsgemeinschaft) and Verband der Chemischen Industrie e.V. (VCI)

Notes

The authors declare no competing financial interest.

Biographies

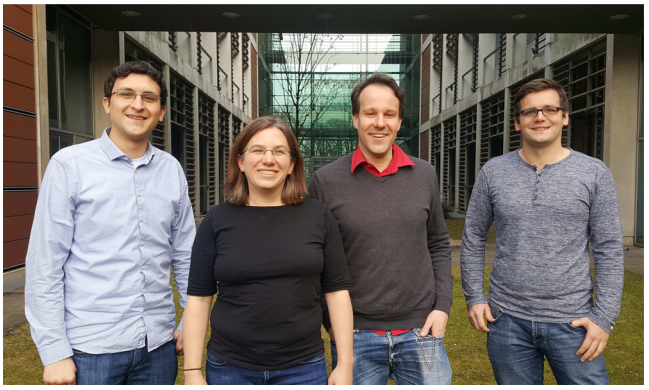

From left to right: Pascal Hebbeker, Stefanie Schneider, Felix A. Plamper, and Alexander A. Steinschulte

Pascal Hebbeker received his M.Sc. in chemistry in 2014 after studying at RWTH Aachen University, Germany, and at Lund University, Sweden. Currently, he is a Ph.D. candidate at the RWTH Aachen University with a scholarship from the Verband der Chemischen Industrie e.V. (VCI). His research interests include the simulation of polymeric systems undergoing complexation.

Stefanie Schneider studied chemistry at the Carl von Ossietzky University of Oldenburg, Germany. For her Ph.D. thesis under the supervision of Per Linse, she joined the Department of Physical Chemistry at Lund University, Sweden. She returned to Germany for a postdoctoral stay at the Research Center Jülich and is now working at the RWTH Aachen University, Germany. Her main research interest is the molecular modeling and simulation of polymer systems.

Felix A. Plamper studied chemistry at the University of Bayreuth, Germany, and at Lund University, Sweden. After his Ph.D. under the supervision of Axel Müller (Bayreuth), he joined Heikki Tenhu's group in 2007 for a postdoctoral stay at the University of Helsinki, Finland. He completed his habilitation at the RWTH Aachen University, Germany, becoming a docent in 2015. His main interest is in complexation phenomena in polymeric systems. He was awarded several scholarships and prizes (such as the Young Scientist Prize of the German Chemical Society - GDCh-Fachgruppe Makromolekulare Chemie).

Alexander A. Steinschulte received his M.Sc. in chemistry at the RWTH Aachen University in 2012. Currently, he is working as a Ph.D. student on the inter- and intramolecular complexation of copolymers in Dr. Felix Plamper's group.

ACKNOWLEDGMENTS

We thank Walter Richtering for continuous support and Tom Breuer for his help with the 3D design of the cover image. Furthermore, funding by Fonds der Chemischen Industrie (FCI) for a scholarship (P.H.) and by the German Research Foundation (DFG, project PL 571/3-2) is gratefully acknowledged.

REFERENCES

(1) Ren, C.-l.; Nap, R. J.; Szleifer, I. The Role of Hydrogen Bonding in Tethered Polymer Layers. *J. Phys. Chem. B* **2008**, *112* (50), 16238−16248.

(2) Nagai, S.; Itou, A.; Patcharat, W.; Yamada, K.; Leong, Y. W.; Hamada, H. Miscibility of polyoxymethylene and poly(lactic acid). *Annu. Technol. Conf.-Soc. Plast. Eng.* **2011**, *69* (1), 47−51.

(3) Hackelbusch, S.; Rossow, T.; van Assenbergh, P.; Seiffert, S. Chain Dynamics in Supramolecular Polymer Networks. *Macromolecules* **2013**, *46* (15), 6273−6286.

(4) Woodward, P. J.; Hermida Merino, D.; Greenland, B. W.; Hamley, I. W.; Light, Z.; Slark, A. T.; Hayes, W. Hydrogen Bonded Supramolecular Elastomers: Correlating Hydrogen Bonding Strength with Morphology and Rheology. *Macromolecules* **2010**, *43* (5), 2512−2517.

(5) Lin, C.-T.; Kuo, S.-W.; Huang, C.-F.; Chang, F.-C. Glass transition temperature enhancement of PMMA through copolymerization with PMAAM and PTCM mediated by hydrogen bonding. *Polymer* **2010**, *51* (4), 883−889.

(6) Sybachin, A. V.; Zaborova, O. V.; Pergushov, D. V.; Zezin, A. B.; Plamper, F. A.; Müller, A. H. E.; Kesselman, E.; Schmidt, J.; Talmon, Y.; Menger, F. M.; Yaroslavov, A. A. Complexes of star-shaped cationic polyelectrolytes with anionic liposomes: Towards multi-liposomal assemblies with controllable stability. *Polymer* **2016**, *93*, 198−203.

(7) Mergel, O.; Wünnemann, P.; Simon, U.; Böker, A.; Plamper, F. A. Microgel Size Modulation by Electrochemical Switching. *Chem. Mater.* **2015**, *27* (21), 7306−7312.

(8) Maccarrone, S.; Mergel, O.; Plamper, F. A.; Holderer, O.; Richter, D. Electrostatic Effects on the Internal Dynamics of Redox-Sensitive Microgel Systems. *Macromolecules* **2016**, *49* (5), 1911−1917.

(9) Mergel, O.; Gelissen, A. P. H.; Wünnemann, P.; Böker, A.; Simon, U.; Plamper, F. A. Selective Packaging of Ferricyanide within

DOI: 10.1021/acs.langmuir.6b04602
Langmuir 2017, 33, 4091−4106

Thermoresponsive Microgels. *J. Phys. Chem. C* **2014**, *118* (45), 26199−26211.
(10) Yaroslavov, A. A.; Sybachin, A. V.; Zaborova, O. V.; Pergushov, D. V.; Zezin, A. B.; Melik-Nubarov, N. S.; Plamper, F. A.; Müller, A. H. E.; Menger, F. M. Electrostatically Driven Complexation of Liposomes with a Star-Shaped Polyelectrolyte to Low-Toxicity Multi-Liposomal Assemblies. *Macromol. Biosci.* **2014**, *14* (4), 491−495.
(11) Plamper, F. A.; Murtomäki, L.; Walther, A.; Kontturi, K.; Tenhu, H. e-Micellization: Electrochemical, Reversible Switching of Polymer Aggregation. *Macromolecules* **2009**, *42* (19), 7254−7257.
(12) Plamper, F. A.; McKee, J. R.; Laukkanen, A.; Nykänen, A.; Walther, A.; Ruokolainen, J.; Aseyev, V.; Tenhu, H. Miktoarm stars of poly(ethylene oxide) and poly(dimethylaminoethyl methacrylate): manipulation of micellization by temperature and light. *Soft Matter* **2009**, *5* (9), 1812−1821.
(13) Plamper, F. A.; Schmalz, A.; Ballauff, M.; Müller, A. H. E. Tuning the Thermoresponsiveness of Weak Polyelectrolytes by pH and Light: Lower and Upper Critical-Solution Temperature of Poly(*N*,*N*-dimethylaminoethyl methacrylate). *J. Am. Chem. Soc.* **2007**, *129* (47), 14538−14539.
(14) Plamper, F. A.; Walther, A.; Müller, A. H. E.; Ballauff, M. Nanoblossoms: Light-Induced Conformational Changes of Cationic Polyelectrolyte Stars in the Presence of Multivalent Counterions. *Nano Lett.* **2007**, *7* (1), 167−171.
(15) Wünnemann, P.; Noyong, M.; Kreuels, K.; Brüx, R.; Gordiichuk, P.; van Rijn, P.; Plamper, F. A.; Simon, U.; Böker, A. Microstructured Hydrogel Templates for the Formation of Conductive Gold Nanowire Arrays. *Macromol. Rapid Commun.* **2016**, *37* (17), 1446−1452.
(16) Mergel, O.; Kühn, P. T.; Schneider, S.; Simon, U.; Plamper, F. A. Influence of Polymer Architecture on the Electrochemical Deposition of Polyelectrolytes. *Electrochim. Acta* **2017**, DOI: 10.1016/j.electacta.2017.02.102.
(17) Hofmann, C. H.; Grobelny, S.; Panek, P. T.; Heinen, L. K. M.; Wiegand, A.-K.; Plamper, F. A.; Jacob, C. R.; Winter, R.; Richtering, W. Methanol-induced change of the mechanism of the temperature- and pressure-induced collapse of N-Substituted acrylamide copolymers. *J. Polym. Sci., Part B: Polym. Phys.* **2015**, *53* (7), 532−544.
(18) Hofmann, C. H.; Plamper, F. A.; Scherzinger, C.; Hietala, S.; Richtering, W. Cononsolvency Revisited: Solvent Entrapment by *N*-Isopropylacrylamide and *N*,*N*-Diethylacrylamide Microgels in Different Water/Methanol Mixtures. *Macromolecules* **2013**, *46* (2), 523−532.
(19) Flory, P. J. Thermodynamics of high-polymer solutions. *J. Chem. Phys.* **1942**, *10*, 51−61.
(20) Shultz, A. R.; Flory, P. J. Phase equilibria in polymer-solvent systems. *J. Am. Chem. Soc.* **1952**, *74*, 4760−7.
(21) Warren, N. J.; Armes, S. P. Polymerization-Induced Self-Assembly of Block Copolymer Nano-objects via RAFT Aqueous Dispersion Polymerization. *J. Am. Chem. Soc.* **2014**, *136* (29), 10174−10185.
(22) Borisov, O. V.; Zhulina, E. B.; Leermakers, F. A. M.; Müller, A. H. E. Self-Assembled Structures of Amphiphilic Ionic Block Copolymers: Theory, Self-Consistent Field Modeling and Experiment. *Adv. Polym. Sci.* **2011**, *241*, 57−129.
(23) Aseyev, V.; Tenhu, H.; Winnik, F. M. Non-ionic Thermoresponsive Polymers in Water. *Adv. Polym. Sci.* **2010**, *242*, 29−89.
(24) Schild, H. G. Poly(*N*-isopropylacrylamide): experiment, theory and application. *Prog. Polym. Sci.* **1992**, *17* (2), 163−249.
(25) Thavanesan, T.; Herbert, C.; Plamper, F. A. Insight in the Phase Separation Peculiarities of Poly(dialkylaminoethyl methacrylate)s. *Langmuir* **2014**, *30* (19), 5609−5619.
(26) Vesterinen, A.; Lipponen, S.; Rich, J.; Seppälä, J. Effect of block composition on thermal properties and melt viscosity of poly[2-(dimethylamino)ethyl methacrylate], poly(ethylene oxide) and poly(propylene oxide) block co-polymers. *eXPRESS Polym. Lett.* **2011**, *5* (9), 754−765.
(27) Zhao, W.; Wang, Y. Coacervation with surfactants: From single-chain surfactants to gemini surfactants. *Adv. Colloid Interface Sci.* **2017**, *239*, 199−212.
(28) Pergushov, D. V.; Müller, A. H. E.; Schacher, F. H. Micellar interpolyelectrolyte complexes. *Chem. Soc. Rev.* **2012**, *41* (21), 6888−6901.
(29) Dähling, C.; Lotze, G.; Drechsler, M.; Mori, H.; Pergushov, D. V.; Plamper, F. A. Temperature-induced structure switch in thermoresponsive micellar interpolyelectrolyte complexes: toward core-shell-corona and worm-like morphologies. *Soft Matter* **2016**, *12* (23), 5127−5137.
(30) Plamper, F. A.; Gelissen, A. P.; Timper, J.; Wolf, A.; Zezin, A. B.; Richtering, W.; Tenhu, H.; Simon, U.; Mayer, J.; Borisov, O. V.; Pergushov, D. V. Spontaneous Assembly of Miktoarm Stars into Vesicular Interpolyelectrolyte Complexes. *Macromol. Rapid Commun.* **2013**, *34* (10), 855−860.
(31) Gelissen, A. P. H.; Pergushov, D. V.; Plamper, F. A. Janus-like interpolyelectrolyte complexes based on miktoarm stars. *Polymer* **2013**, *54* (26), 6877−6881.
(32) Gelissen, A. P. H.; Schmid, A. J.; Plamper, F. A.; Pergushov, D. V.; Richtering, W. Quaternized microgels as soft templates for polyelectrolyte layer-by-layer assemblies. *Polymer* **2014**, *55* (8), 1991−1999.
(33) Pergushov, D. V.; Babin, I. A.; Plamper, F. A.; Zezin, A. B.; Müller, A. H. E. Water-Soluble Complexes of Star-Shaped Poly(acrylic acid) with Quaternized Poly(4-vinylpyridine). *Langmuir* **2008**, *24* (13), 6414−6419.
(34) Sigolaeva, L. V.; Gladyr, S. Y.; Gelissen, A. P. H.; Mergel, O.; Pergushov, D. V.; Kurochkin, I. N.; Plamper, F. A.; Richtering, W. Dual-Stimuli-Sensitive Microgels as a Tool for Stimulated Spongelike Adsorption of Biomaterials for Biosensor Applications. *Biomacromolecules* **2014**, *15* (10), 3735−3745.
(35) Sigolaeva, L. V.; Mergel, O.; Evtushenko, E. G.; Gladyr, S. Y.; Gelissen, A. P. H.; Pergushov, D. V.; Kurochkin, I. N.; Plamper, F. A.; Richtering, W. Engineering systems with spatially-separated enzymes via dual-stimuli-sensitive properties of microgels. *Langmuir* **2015**, *31* (47), 13029−13039.
(36) Bailey, F. E.; Lundberg, R. D.; Callard, R. W. Some factors affecting the molecular association of poly(ethylene oxide) and poly(acrylic acid) in aqueous solution. *J. Polym. Sci., Part A: Gen. Pap.* **1964**, *2* (2), 845−851.
(37) Dobry, M. A. Sur l'incompatibilité des macromolécules en solution aqueuse. *Bull. Soc. Chim. Belg.* **1948**, *57* (7−9), 280−285.
(38) Mano, V.; E Silva, M. E. S. R.; Barbani, N.; Giusti, P. Binary blends based on poly(*N*-isopropylacrylamide): miscibility studies with PVA, PVP, and PAA. *J. Appl. Polym. Sci.* **2004**, *92* (2), 743−748.
(39) Ruiz-Rubio, L.; Laza, J. M.; Pérez, L.; Rioja, N.; Bilbao, E. Polymer−polymer complexes of poly(*N*-isopropylacrylamide) and poly(*N*,*N*-diethylacrylamide) with poly(carboxylic acids): a comparative study. *Colloid Polym. Sci.* **2014**, *292* (2), 423−430.
(40) Maeda, Y.; Yamabe, M. A unique phase behavior of random copolymer of *N*-isopropylacrylamide and *N*,*N*-diethylacrylamide in water. *Polymer* **2009**, *50* (2), 519−523.
(41) Hou, L.; Wu, P. Comparison of LCST-transitions of homopolymer mixture, diblock and statistical copolymers of NIPAM and VCL in water. *Soft Matter* **2015**, *11* (14), 2771−2781.
(42) Frieberg, B.; Kim, J.; Narayanan, S.; Green, P. F. Surface Dynamics of Miscible Polymer Blend Nanocomposites. *ACS Nano* **2014**, *8* (1), 607−613.
(43) Tomba, J. P.; Carella, J. M.; Pastor, J. M. Molecular Mechanisms of Interphase Evolution in the Liquid Polystyrene−Glassy Poly(phenylene oxide) System. *Macromolecules* **2009**, *42* (10), 3565−3572.
(44) Sharma, M.; Madras, G.; Bose, S. Shear-induced crystallization in different polymorphic forms of PVDF induced by surface functionalized MWNTs in PVDF/PMMA blends. *Phys. Chem. Chem. Phys.* **2014**, *16* (31), 16492−16501.
(45) Spruijt, E.; Westphal, A. H.; Borst, J. W.; Cohen Stuart, M. A.; van der Gucht, J. Binodal Compositions of Polyelectrolyte Complexes. *Macromolecules* **2010**, *43* (15), 6476−6484.
(46) Schilli, C. M.; Zhang, M.; Rizzardo, E.; Thang, S. H.; Chong, Y. K.; Edwards, K.; Karlsson, G.; Müller, A. H. E. A New Double-Responsive Block Copolymer Synthesized via RAFT Polymerization:

DOI: 10.1021/acs.langmuir.6b04602
Langmuir 2017, 33, 4091−4106

Poly(*N*-isopropylacrylamide)-block-poly(acrylic acid). *Macromolecules* **2004**, *37* (21), 7861−7866.
(47) Steinschulte, A. A.; Schulte, B.; Erberich, M.; Borisov, O. V.; Plamper, F. A. Unimolecular Janus Micelles by Microenvironment-Induced, Internal Complexation. *ACS Macro Lett.* **2012**, *1* (4), 504−507.
(48) Hatada, K.; Kitayama, T.; Ute, K.; Nishiura, T. Preparation of uniform stereoregular polymer, stereoblock polymer, and copolymer of methacrylate and their stereocomplex formation. *Macromol. Symp.* **1998**, *132*, 221−230.
(49) Tsuji, H. Poly(lactide) stereocomplexes: Formation, structure, properties, degradation, and applications. *Macromol. Biosci.* **2005**, *5* (7), 569−597.
(50) Whitmore, M. D.; Vavasour, J. D.; Spiro, J. G.; Winnik, M. A. On Cylindrical PS-b-PMMA in Moderate and Weak Segregation. *Macromolecules* **2013**, *46* (22), 9045−9054.
(51) Rahman, S. S. A.; Kawaguchi, D.; Matsushita, Y. Microphase-Separated Structures of Poly(4-*tert*-butylstyrene-block-4-tert-butoxystyrene) upon Gradual Changes in Segregation Strength through Hydrolysis Reaction. *Macromolecules* **2011**, *44* (8), 2799−2807.
(52) Li, Z.; Kesselman, E.; Talmon, Y.; Hillmyer Marc, A.; Lodge Timothy, P. Multicompartment micelles from ABC miktoarm stars in water. *Science* **2004**, *306* (5693), 98−101.
(53) Schacher, F.; Walther, A.; Müller, A. H. E. Dynamic Multicompartment-Core Micelles in Aqueous Media. *Langmuir* **2009**, *25* (18), 10962−10969.
(54) Betthausen, E.; Drechsler, M.; Fortsch, M.; Schacher, F. H.; Muller, A. H. E. Dual stimuli-responsive multicompartment micelles from triblock terpolymers with tunable hydrophilicity. *Soft Matter* **2011**, *7* (19), 8880−8891.
(55) Rinkenauer, A. C.; Schallon, A.; Günther, U.; Wagner, M.; Betthausen, E.; Schubert, U. S.; Schacher, F. H. A Paradigm Change: Efficient Transfection of Human Leukemia Cells by Stimuli-Responsive Multicompartment Micelles. *ACS Nano* **2013**, *7* (11), 9621−9631.
(56) Löbling, T. I.; Haataja, J. S.; Synatschke, C. V.; Schacher, F. H.; Müller, M.; Hanisch, A.; Gröschel, A. H.; Müller, A. H. E. Hidden Structural Features of Multicompartment Micelles Revealed by Cryogenic Transmission Electron Tomography. *ACS Nano* **2014**, *8* (11), 11330−11340.
(57) Israelachvili, J. N.; Mitchell, D. J.; Ninham, B. W. Theory of self-assembly of lipid bilayers and vesicles. *Biochim. Biophys. Acta, Biomembr.* **1977**, *470* (2), 185−201.
(58) Hebbeker, P.; Linse, P.; Schneider, S. Optimal Displacement Parameters in Monte Carlo Simulations. *J. Chem. Theory Comput.* **2016**, *12* (4), 1459−1465.
(59) Hebbeker, P.; Plamper, F. A.; Schneider, S. Effect of the Molecular Architecture on the Internal Complexation Behavior of Linear Copolymers and Miktoarm Star Polymers. *Macromol. Theory Simul.* **2015**, *24* (2), 110−116.
(60) Steinschulte, A.; Xu, W.; Draber, F.; Hebbeker, P.; Jung, A.; Bogdanovski, D.; Schneider, S.; Tsukruk, V. V.; Plamper, F. A. Interface-Enforced Complexation between Copolymer Blocks. *Soft Matter* **2015**, *11* (18), 3559−3565.
(61) Müller, A. H. E.; Wooley, K. L. In *Polymer Science: A Comprehensive Reference*; Matyjaszewski, K., Möller, M., Eds.; Elsevier: Amsterdam, 2012; Chapter 6.01, pp 1−4.
(62) Miquelard-Garnier, G.; Roland, S. Beware of the Flory parameter to characterize polymer-polymer interactions: A critical reexamination of the experimental literature. *Eur. Polym. J.* **2016**, *84*, 111−124.
(63) Eckelt, J.; Samadi, F.; Wurm, F.; Frey, H.; Wolf, B. A. Branched Versus Linear Polyisoprene: Flory-Huggins Interaction Parameters for their Solutions in Cyclohexane. *Macromol. Chem. Phys.* **2009**, *210* (17), 1433−1439.
(64) Hildebrand, J. H. Factors determining solubility among nonelectrolytes. *Proc. Natl. Acad. Sci. U. S. A.* **1950**, *36*, 7−15.
(65) Hansen, C. M. *Three Dimension Solubility Parameter and Solvent Diffusion Coefficient: Their Importance in Surface Coating Formulation*; Danish Technical Press: Copenhagen, 1967; p 106.
(66) Peretti, K. L.; Ajiro, H.; Cohen, C. T.; Lobkovsky, E. B.; Coates, G. W. A Highly Active, Isospecific Cobalt Catalyst for Propylene Oxide Polymerization. *J. Am. Chem. Soc.* **2005**, *127* (33), 11566−11567.
(67) Firman, P.; Kahlweit, M. Phase behavior of the ternary system water-oil - polypropylene glycol (PPG). *Colloid Polym. Sci.* **1986**, *264* (11), 936−42.
(68) Hoy, K. L. New values of the solubility parameters from vapor pressure data. *J. Paint Technol.* **1970**, *42* (541), 76−118.
(69) Yamamoto, H. Hansen Solubility Parameters Application Notes https://pirika.com/NewHP/PirikaE/polymer-solvent.html (accessed December 22, 2016).
(70) Morales, E.; Acosta, J. L. Polymer Solubility Parameters of Poly(propylene oxide) Rubber from Inverse Gas Chromatography Measurements. *Polym. J.* **1996**, *28* (2), 127−130.
(71) Yazici, D. T.; Askin, A.; Bütün, V. Thermodynamic interactions of water-soluble homopolymers and double-hydrophilic diblock copolymer. *J. Chem. Thermodyn.* **2008**, *40* (3), 353−361.
(72) Hoy, K. L. Solubility parameter as a design parameter for water borne polymers and coatings. *J. Ind. Text.* **1989**, *19*, 53−76.
(73) Lechner, M. D.; Gehrke, K.; Nordmeier, E. H. *Makromolekulare Chemie*; Birkhäuser Verlag: Basel, 1996; pp 361−368.
(74) Plamper, F. A.; Steinschulte, A. A.; Hofmann, C. H.; Drude, N.; Mergel, O.; Herbert, C.; Erberich, M.; Schulte, B.; Winter, R.; Richtering, W. Toward Copolymers with Ideal Thermosensitivity: Solution Properties of Linear, Well-Defined Polymers of *N*-Isopropyl Acrylamide and *N*,*N*-Diethyl Acrylamide. *Macromolecules* **2012**, *45* (19), 8021−8026.
(75) Steinschulte, A. A.; Schulte, B.; Rütten, S.; Eckert, T.; Okuda, J.; Möller, M.; Schneider, S.; Borisov, O. V.; Plamper, F. A. Effects of Architecture on the Stability of Thermosensitive Unimolecular Micelles. *Phys. Chem. Chem. Phys.* **2014**, *16* (10), 4917−4932.
(76) Ono, Y.; Shikata, T. Hydration and Dynamic Behavior of Poly(N-isopropylacrylamide)s in Aqueous Solution: A Sharp Phase Transition at the Lower Critical Solution Temperature. *J. Am. Chem. Soc.* **2006**, *128* (31), 10030−10031.
(77) Seuring, J.; Agarwal, S. Polymers with Upper Critical Solution Temperature in Aqueous Solution: Unexpected Properties from Known Building Blocks. *ACS Macro Lett.* **2013**, *2* (7), 597−600.
(78) Keerl, M.; Richtering, W. Synergistic depression of volume phase transition temperature in copolymer microgels. *Colloid Polym. Sci.* **2007**, *285* (4), 471−474.
(79) Ito, S. Phase transition of aqueous solution of poly(*N*-alkylacrylamide) derivatives. Effects of side chain structure. *Kobunshi Ronbunshu* **1989**, *46* (7), 437−43.
(80) Keerl, M.; Smirnovas, V.; Winter, R.; Richtering, W. Interplay between hydrogen bonding and macromolecular architecture leading to unusual phase behavior in thermosensitive microgels. *Angew. Chem., Int. Ed.* **2008**, *47* (2), 338−341.
(81) Plamper, F. A.; Reinicke, S.; Elomaa, M.; Schmalz, H.; Tenhu, H. Pearl Necklace Architecture: New Threaded Star-Shaped Copolymers. *Macromolecules* **2010**, *43* (5), 2190−2203.
(82) Steinschulte, A.; Schulte, B.; Drude, N.; Erberich, M.; Herbert, C.; Okuda, J.; Möller, M.; Plamper, F. A Nondestructive, Statistical Method for Determination of Initiation Efficiency: Dipentaerythritol-Aided Synthesis of Ternary ABC_3 Miktoarm Stars using a Combined "Arm-First" and "Core-First" Approach. *Polym. Chem.* **2013**, *4* (13), 3885−3895.
(83) Khanna, K.; Varshney, S.; Kakkar, A. Miktoarm star polymers: advances in synthesis, self-assembly, and applications. *Polym. Chem.* **2010**, *1* (8), 1171−1185.
(84) Petrov, P.; Tsvetanov, C. B.; Jerome, R. Stabilized Mixed Micelles with a Temperature-Responsive Core and a Functional Shell. *J. Phys. Chem. B* **2009**, *113* (21), 7527−7533.
(85) Tan, W. S.; Cohen, R. E.; Rubner, M. F.; Sukhishvili, S. A. Temperature-Induced, Reversible Swelling Transitions in Multilayers

DOI: 10.1021/acs.langmuir.6b04602
Langmuir 2017, 33, 4091−4106

of a Cationic Triblock Copolymer and a Polyacid. *Macromolecules* **2010**, *43* (4), 1950−1957.
(86) Grosberg, A.; Nechaev, S. *Polymer Characteristics*; Advances in Polymer Science; Springer-Verlag: Berlin, 1993; Vol. *106*, Polymer Topology, pp 1−29; DOI: 10.1007/BFb0025860.
(87) Kim, Y. H.; Webster, O. W. Hyperbranched polyphenylenes. *Macromolecules* **1992**, *25* (21), 5561−5572.
(88) Tsuji, H.; Suzuki, M. Hetero-Stereocomplex Crystallization between Star-Shaped 4-Arm Poly(l-2-hydroxybutanoic acid) and Poly(d-lactic acid) from the Melt. *Macromol. Chem. Phys.* **2014**, *215* (19), 1879−1888.
(89) Plamper, F. A.; Ruppel, M.; Schmalz, A.; Borisov, O.; Ballauff, M.; Müller, A. H. E. Tuning the Thermoresponsive Properties of Weak Polyelectrolytes: Aqueous Solutions of Star-Shaped and Linear Poly(*N*,*N*-dimethylaminoethyl Methacrylate). *Macromolecules* **2007**, *40* (23), 8361−8366.
(90) Virtanen, J.; Lemmetyinen, H.; Tenhu, H. Fluorescence and EPR studies on the collapse of poly(*N*-isopropyl acrylamide)-g-poly(ethylene oxide) in water. *Polymer* **2001**, *42* (23), 9487−9493.
(91) van't Hoff, J. H. *Studies in Chemical Dynamics*; F. Muller: Amsterdam, 1896.
(92) Loh, X. J. Poly(dimethylaminoethyl methacrylate-co-propylene glycol methacrylate): Dual-responsive "reversible" micelles. *J. Appl. Polym. Sci.* **2013**, *127* (2), 992−1000.
(93) Hebbeker, P.; Steinschulte, A. A.; Schneider, S.; Okuda, J.; Möller, M.; Plamper, F. A.; Schneider, S. Complexation in Weakly Attractive Copolymers with Varying Composition and Topology: Linking Fluorescence Experiments and Molecular Monte Carlo Simulations. *Macromolecules* **2016**, *49* (22), 8748−8757.
(94) Casse, O.; Shkilnyy, A.; Linders, J.; Mayer, C.; Haussinger, D.; Völkel, A.; Thünemann, A. F.; Dimova, R.; Cölfen, H.; Meier, W.; Schlaad, H.; Taubert, A. Solution Behavior of Double-Hydrophilic Block Copolymers in Dilute Aqueous Solution. *Macromolecules* **2012**, *45* (11), 4772−4777.
(95) Polikt, W. F.; Burchard, W. Static Light Scattering from Aqueous Poly(ethylene oxide) Solutions in the Temperature Range 20−90 °C. *Macromolecules* **1983**, *16*, 978−982.
(96) Doty, P. M.; Zimm, B. H.; Mark, H. Some light-scattering experiments with high-polymer solutions. *J. Chem. Phys.* **1944**, *12*, 144−5.
(97) Turro, N. J.; Yekta, A. Luminescent probes for detergent solutions. A simple procedure for determination of the mean aggregation number of micelles. *J. Am. Chem. Soc.* **1978**, *100* (18), 5951−2.
(98) Pottier, C.; Morandi, G.; Rihouey, C.; Dulong, V.; Picton, L.; Le Cerf, D. Thermosensitive behavior of amphiphilic triblock copolymers based on poly(acrylic acid) and poly(propylene oxide). *J. Polym. Sci., Part B: Polym. Phys.* **2016**, *54* (15), 1507−1514.
(99) Han, X.; Zhang, X.; Zhu, H.; Yin, Q.; Liu, H.; Hu, Y. Effect of Composition of PDMAEMA-b-PAA Block Copolymers on Their pH- and Temperature-Responsive Behaviors. *Langmuir* **2013**, *29* (4), 1024−1034.
(100) Plamper, F. A.; Richtering, W. Functional Microgels and Microgel Systems. *Acc. Chem. Res.* **2017**, *50* (2), 131−140.

DOI: 10.1021/acs.langmuir.6b04602
Langmuir 2017, 33, 4091−4106